Biointerface Research in Applied Chemistry
Open-Access Journal (ISSN: 2069-5837)

Article
Volume 16, Issue 2, 2026, 59
https://doi.org/10.33263/BRIAC162.059

Experimental Study and Numerical Calculations to Increase the Electricity Generation of Microbial Fuel Cells (MFCs): A Comparison for Creating Voltages using Various Bacteria from Waste Materials

Majid Monajjemi [1,*], Fatemeh Mollaamin [2], Mersedeh. Rahpayma [3], Elnaz Fakhraian [4]

[1] Department of Biology, Faculty of Science, Kastamonu University, Kastamonu 37100, Turkey.
[2] Department of Biomedical Engineering, Faculty of Engineering and Architecture, Kastamonu University, Kastamonu 37150, Turkey.
[3] Department of Dentistry, Faculty of Dentistry, Kocaeli Health and Technology University, Kocaeli, Turkey.
[4] Department of Chemical Engineering, Science and Research branch, Islamic Azad University, Tehran, Iran.
* Correspondence: m_monajjemi@yahoo.com;

Received: 11.06.2025; Accepted: 27.10.2026; Published: 15.04.2026

Abstract: MFC is a significant devices that enable the generation of electricity through anaerobic fermentation of waste materials using microbes as bio-catalysts. Since this work focuses on the electricity production of microbial fuel cells (MFCs) of various bacteria from waste materials, we studied the efficiency of industrial waste materials and soil composition containing several bacteria, including *E. coli*, *Shewanella putrefaciens*, *Geobacter sulfurreducens*, and *Lactobacillus*, that are able to create large amounts of suitable electrical power through the MFC. We followed two main approaches in this work: first, testing the efficiency of MFCs, such as the percentage of organic matter in each sample; and second, evaluating the electrical capacity of MFCs due to thermal limits. To study the process performance, the effects of temperature, structures, dimensions, and the distance between the cathodic and anodic chambers on the electrical power were investigated, and the amperage and voltage outputs from electrochemical and microbial cells were recorded. Additionally, in this work, we modeled a steady state using mathematical simulation based on mass, charge, and energy balances for MFCs. The data obtained from the numerical calculation matched our experimental results exactly. Finally, in contrast to most MFC work, which has long-term targets for renewable energy from wastewater, this study can be used immediately in practice. This work also confirms that the electricity production of MFCs can be increased by selecting appropriate conditions for sample type, temperature, and chamber size.

Keywords: microbial fuel cell (MFC); industrial wastewater; proton exchange membranes (PEM); sustainable energy source; renewable electricity production capacity; numerical calculations.

1. Introduction

1.1. MFCs in the new world of global warming.

In a globalized world, humans need more energy due to climate change and global warming. In the present era, most energy comes from petroleum, a non-renewable resource. Therefore, to address this problem, scientists seek new, sustainable, renewable, and alternative

energy sources [1-5]. Consequently, an electrochemical reaction in an MFC occurs at a solid conducting electrode using pollutant substrates from waste as the origin fuels. Wastewater effluents can serve as a source of food for microorganisms during cellular respiration, thereby causing an electron transfer from microorganisms to the electrode surface [6]. Such features enhance electrical power performance by increasing the electron transfer rate in electrochemical reactions [7]. Therefore, one of the objectives of this work is to identify suitable nanomaterials for generating energy from various waste products of microorganisms [8]. Obviously, rich waste matters from waste effluents for producing clean energy in big cities, in the presence of electroactive microorganisms, are a major necessity for the ecosystem [9]. In addition, chemical substrate degradation of waste matter with multifunctional nanomaterial in the presence of electroactive microorganisms is another purposeful strategy in our research for simultaneous waste treatment and electricity generation. Hence, waste management in the commercial context makes MFC a sustainable alternative sector of renewable energy [9-12].

1.2. Structure and configuration of MFCs.

MFC consists of two chambers (anode and cathode) that are separated by a salt bridge. The opening of the salt bridge was blocked with cotton so that the solutions of the anode and cathode could not mix with each other. Electrons move through membrane-bound quinone and cytochrome via mediators such as methylene blue. The electrons move from the anode to the cathode through the external circuit, whereas protons move through the salt bridge, which is known as a proton exchange membrane (PEM). Reduction occurs at the cathode in the presence of oxygen, and the protons form water in the cathodic chamber. Hence, the bacteria form CO_2 and H_2O during the decomposition of substrate, and therefore, because of oxygen's role as an inhibitor, the anode chambers should be made Anaerobic. Since the anode chamber is anaerobic and the cathode chamber can be aerobic, the cathode electrode can be omitted, resulting in a single-compartment MFC (Figure 1). For instance, in using acetate as a substrate, the cathodic and anodic reactions are as follows.

$$\text{Anodic reaction: } C_2H_4O_2+2H_2O \rightarrow 2CO_2 + 8e^- + 8H^+ \quad (1)$$

$$\text{Cathodic reaction: } 2O_2+8e^- + 8H^+ \rightarrow 4H_2O \quad (2)$$

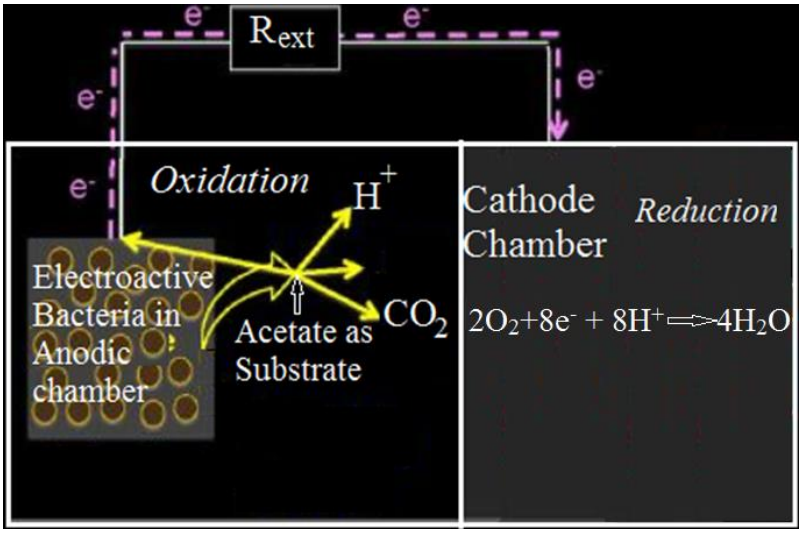

Figure 1. Acetate as a substrate with cathodic and anodic reactions.

The performance of MFC can be estimated using the power density parameter and the electrical current intensity. Since MFC is a function of many variables, multidisciplinary subjects and various fields would benefit from the best possible optimization. In this work for the MFC model, we focused mostly on nanomaterials for electrodes, Substrates, and various electrogenic microorganisms.

1.3. Electroactive microorganism.

Although pollutants are removed from contaminated areas by microorganisms, which are essential to nature, even with advanced technology, the challenge is the limited contact between pollutants and microbes [12-14]. Therefore, to select appropriate pollutants, an accurate assessment of unattainable residual contaminant levels with low yields is needed, and, accordingly, transition metal oxide nanocatalysts are a suitable indicator for this purpose [15, 16]. Because bacteria can transfer electron potential and form a slimy biofilm, they are known as electrochemically active bacteria (EAB). EAB is a novel subject for converting the chemical energy to electrical energy through bioremediation technology [17]. Biofilms are communities of electroactive microorganisms that are supported by extracellular compounds, including polysaccharides, proteins, and nucleic acids, located outside the cells of the microorganisms. These biofilms increase the conducting electrode with surfaces of bacterial cell attachment [18]. Because microbes harbor hazardous molecules, bacteria can degrade waste compounds for energy and a carbon source to survive in their life cycle [19]. *Escherichia coli*, Shewanella putrefaciens, and Geobacter sulfurreducens can produce electrons within the cell and then transfer them to extracellular acceptors via cytochromes and biofilms. These batteries exhibit sufficient columbic performance as acceptors in biofilms on the electrode surface and can transfer electrons directly to the anode, thereby increasing energy production [20].

2. Materials and Methods

2.1. MFC construction.

Our MFC system (Figure 2) is made of 1- Anode chamber that keep the bacteria and organic substrate in an anaerobic media; 2- Cathode chamber that keep a conductive solution of salt; 3- Salt bridge including Proton-exchange membrane for separating the anode and cathode chambers from each other but enable to transit the protons from anodic chamber to cathodic chamber; 4- External circuit for transit the electrons towards cathode chamber as well as a path for electrons for pulling out from the anode.

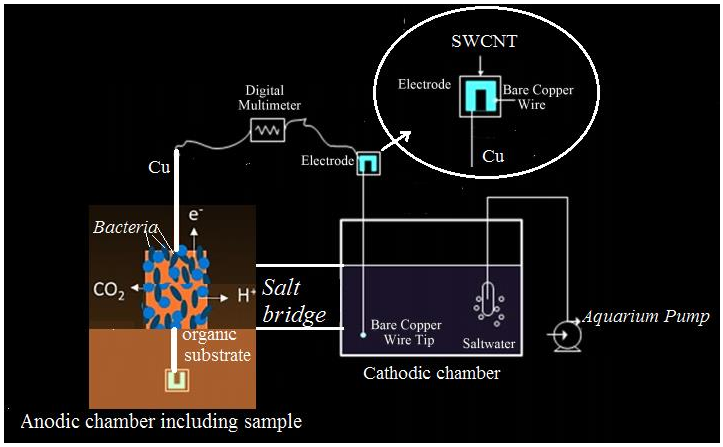

Figure 2. Schematic of MFC system setup, including cathodic and anodic chambers.

During oxidation as part of their metabolic activity, bacteria produce protons and electrons that are pulled out of solution at the anode through circuit wires and deposited on a related electrode. The electrons are then conducted into the cathode chamber. Since MFC is powered through various bacteria in the anode chamber, we selected several suitable bacteria, including *Escherichia coli*, *Shewanella putrefaciens*, and *Geobacter sulfurreducens*.

2.1.1. Membrane selection.

Membranes in MFCs have a basic character due to the decreasing internal resistance, prevention of pH splitting, and saving costs. It is notable that membrane compounds are generally categorized as cation exchange membrane (CEM), anion exchange membrane (AEM), and we checked and tested any of these types in our experiments [21]. The most commonly applicable membrane is CEM, which is widely used due to its easy proton transfer. We tested both Nafion 115 and Ultrex CMI 7000 and confirmed Nafion 115 because the negatively charged hydrophilic sulfonate group attached to hydrophobic fluorocarbon has the most efficiency in CEM cerise. We also selected Nafion 115 commercial membranes (Dupont Company) in the Na^+-form (Nafion-Na) with dimensions of 100×30 × 0.125 mm. The Nafion-Na membranes exhibited ionic conductivity of 3.52×10^{-4} S cm−1 at 298 K and 1.52×10^{-3} S cm^{-1} at 70°C, respectively [22]. Based on Koók *et al*.'s works, we also connected the cathode chamber to the membrane section for removing impurities and increasing the porosity of the membrane [23]. Before starting the tests, Nafion was prepared by using 5 wt% hydrogen peroxide and 15 wt% sulfuric acid at 80°C for one hour, respectively. The sodium-ion exchange procedure was mixed in 250 ml of NaOH aqueous solution (10 g sodium hydroxide in 250 ml of deionized water) at 80°C for 5 h [21-23]. Since CEM cerise has a major drawback for using CEM in MFC in long-term operations, in other experiments, we used AEM. We proved that the AEM series has an excellent proton transfer rate compared with CEM, due to the structures of phosphate or carbonate. In addition, pH is better balanced in MFC with AEM because of phosphate anions [24]. Table 1 presents a summary of various membranes, and we used Tokuyama: A201 Tokuyama's AEM products from Japan among this list [25-30].

Table 1. Specification of Various membranes, including Tokuyama: A201 Tokuyama's AEM products.

Membrane	**Backbones**	**Transferring functional group**	**Membrane specification (a):Ionic conductivity;(b):IEC; (c)Thickness; (d):Tensile strength; (e): Elongation at break**
Tokuyama: A201 and A901	-	-	(a) 42 mS cm^{-1} (OH^-); (b)1.8 meq/g ; (c) 28 µm; (d) 96 MPa, (e) 62%
Aemion™ series	Methylated polybenzimidazoles	Imidazole	(a)80 mS cm^{-1}; (b)2.1–2.5 meq/g; (c) Depends on the Product chosen; (d) 60MPa; (e) 80-110%
XION™Composite-72-10CL	Poly-norbornene	Pendant quaternary ammonium	(c) 10 µm; (d) No; (a) No; (d) No
PiperION™ Versogene	Poly-aryl Piperidinium	PiPeridine	(a) 150 mS cm^{-1} ($OH^{-;;}$); (b) 1.04meq/g; (c) Depends on the Product chosen;(d) Tensile strength: >30 MPa; (e) Elongation at break>30%
aQAPS-S8	Polysulfon	quaternary ammonium	(a) 54 mS cm^{-1} (OH^-); (b) 1.8 meq/g; (c) 50 µm; (d) No, (e) No
Orion TM1	Poly-terphenylen	Pendant quaternary ammonium	(a) 54 mS cm^{-1} (OH^-); I(b) 2.19 meq/g; (c) 24 µm; (d) 30 MPa; (e) 35%

2.1.2. Preparation of anode chamber.

The anodic chamber is a major part where biomass decomposition occurs inside the electrode to initiate bacterial activity. The performance of an MFC is typically described by measuring the anode efficiency, as it serves as an active center for living bioelectrochemical

activities and mediates electron transport from exoelectrogens to the anodic chamber. Therefore, it is essential to concentrate on the anode materials and design. Several items influence the performance of the MFC, such as bio materials in anodic chambers, bacteria types, and proton transfer membranes. Usually, carbonaceous metal-based compounds are widely used in MFCs, such as carbon paper, carbon rods, carbonized cardboard, and carbon cloth, the last of which is used in the anodic chamber due to its high strength and high porosity, which creates a relatively high surface area [30-35]. In this work, we used various types of carbon cloth as electrodes, which were soaked in distilled water at 298 K for half an hour and then boiled in deionized water for 15 minutes to remove contaminants accumulated within their pores. Three layers of carbon cloth cover the T-shaped anode to achieve an appropriate thickness. We also used several metal plates, mostly stainless steel sheets, for anode materials.

2.1.3. Preparation of cathode chamber.

In the cathodic chamber, electrons reduce oxygen to water via reduction reactions that can occur at three-phase interfaces, including air, liquid, and solid phases. A general cathodic chamber electrode consists of an electrode assist, a special catalyst, and an air diffusion section. Although anodic chamber electrode materials can sometimes be used in the cathodic chamber, it is notable that the cathode material should have higher conductivity and mechanical strength than anodic materials. Mostly MFCs are being worked under neutral PH and mild temperatures. Using expensive transition metals such as platinum, gold, and even silver as catalysts for cathode materials is limiting the practical applications of MFC technology. Therefore, it is necessary to reduce the cost of cathodic catalysts by replacing the cheaper materials with platinum without sacrificing efficiency, such as carbon cloth coated with polytetrafluoroethylene. The MFC efficiency by using carbon cloth coated with poly-tetrafluoroethylene increased the power densities by around 35% compared with a carbon-based one-layered cloth.

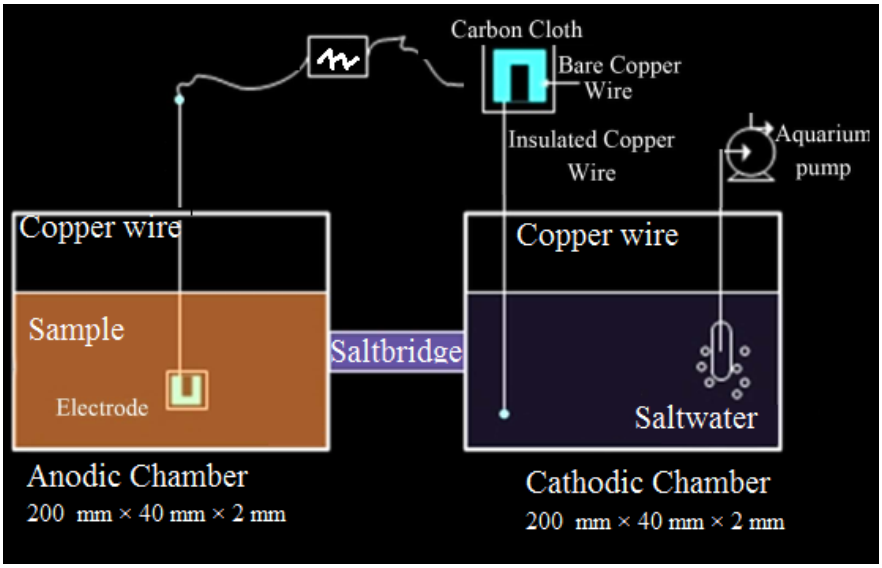

Figure 3. Preparing the cathode chamber, including a salt bridge between the cathode and anode sections.

In this work, we used commercial carbon electrodes due to properties like a wide electrochemical window, low residual current, recyclability, reusability, and sufficient electrical conductivity [36]. In our work, we used a combination platinum-carbon catalyst on the cathode chamber electrode to increase the rate of oxygen recovery and reduce the

overpotential at the cathode. Thus, platinum powder with a 15 wt% loading of 0.20 mg/, water, and ethanol was mixed for half an hour. Next, 50 wt% of the ordinary polymer binder used in the fabrication of metal-carbon composite electrodes, polytetrafluoroethylene (PTFE), was added to make a 40 wt% solution, and the mixture was stirred for 15 minutes. After that, the surface of the air cathode with dimensions 200 mm × 40 mm × 2 mm, as shown in Figure 3, was impregnated with the prepared mixture using a brush.

2.2. Bacterial preparation.

2.2.1. Microbes used.

Microorganisms are the major component of MFC for treatment and electricity generation. Potter in 1911 exhibited that yeast *Saccharomyces cerevisiae* and *Bacillus coli* provided a suitable voltage in electricity generation [37]. So, for increasing the performance of the power output, knowledge of microorganism types from the point of view of properties, qualities, and quantities is needed. The primary activation of bacteria is through colonization of the anode electrode as a bio-catalyst, along with the substrates, to generate electricity. In Table 2, we used four different microorganisms, including *Escherichia coli* bacteria, *Shewanella putrefaciens* bacteria, *Geobacter sulfurreducens*, and *Lactobacillus*, in our MFC study.

Table 2. Different microorganisms are used in MFC.

No	Microorganisms	No	Microorganisms	No	Microorganisms
1	*Geobacter* SPP [38]	9	*Geothrix fermentas* [47]		*Erwinia dissolven* [53]
2	*Geobacter. Sulfurreducens* [39]	10	*Chlorella vugaris* [48]		*Lactobacillus plantarum* [53]
3	*Shewanella oneidensis* [40]	11	*Dunaliealla tertiolecta* [49]		*Paracoccus denitrificans* [53]
4	*Shewanella putrefaciens* [41]	12	*Scenedesmus obliquus* [49]		Paracoccus pantotrophus [54]
5	*Escherichia coli* [42]	13	*Chlorella pyrenoidosa* [50]		*Proteus vulgaris* [54]
6	*Clostridium butyricum* [43,44]	14	*Corilous versicolor* [50]		*Proteus mirabilis* [54]
7	*Pseudomonas aeruginosa* [45,46]	15	*Agaricus meleagris* [51]		
8	*Gluconobacter oxydans* [46]	16	*Streptococcus lactis* [52]		

Escherichia coli is a Gram-negative bacterium, generally used in both research laboratories and teaching centers. For this work, we grow it at 37°C under aerobic conditions.; Since *E. coli* can grow under a wide range of pH, we have grown it in Luria-Bertani broth as a rich liquid broth medium. During an overnight, the cell density of >115 cfu/ml (colony-forming units per milliliter) of culture appeared (Figure 4a). *Shewanella putrefaciens* is a Gram-negative pleomorphic bacterium.

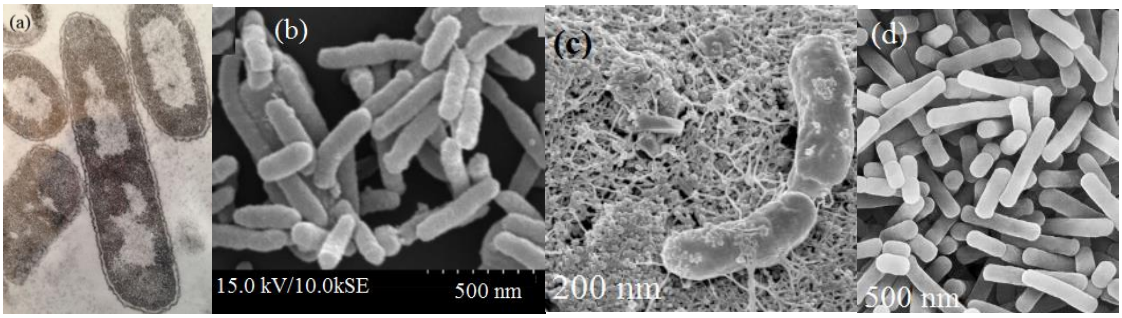

Figure 4. SEM of several bacteria by suitable resolation **(a)** E. coli**; (b)** Shewanella putrefaciens; **(c)** Geobacter sulfurreducens; **(d)** Lactobacillus.

We isolated it from the Caspian Sea. *Geobacter sulfurreducens* is a Gram-negative metal- and sulfur-reducing proteobacterium. It is a rod-shaped, aerotolerant anaerobe that is

non-fermentative, has a flagellum, and type four pili. It is closely related to *Geobacter metallireducens*. *Geobacter sulfurreducens* is an anaerobic species of bacteria that belongs to the family Geobacteraceae. *Lactobacillus* is a genus of Gram-positive facultative anaerobic or microaerophilic bacteria. *Lactobacillus* is a genus of Gram-positive facultative anaerobic or microaerophilic bacteria. The genus *Lactobacillus* is one of the major subgroups of the lactic acid bacteria, which convert lactose and other sugars into lactic acid. They are widely distributed and generally benign. They are found in humans as a small part of the natural flora, symbiotically present in the vagina and gastrointestinal tract.

2.3. Experimental procedure.

2.3.1. Morphological and biochemical characterization.

Morphological characteristics, Gram staining, several biochemical tests, and an online software (ABIS)- based approach were used for the identification of potential electrogenic bacteria.

2.3.2. Mass transport calculations and numerical analysis.

Initially, the air-cathode membrane was simulated without an MFC using a steady-state two-dimensional model. This model coupled bio-electrochemical kinetics with mass, charge, and heat transfer [12]. A schematic image of the modeling details is shown in Figure 5.

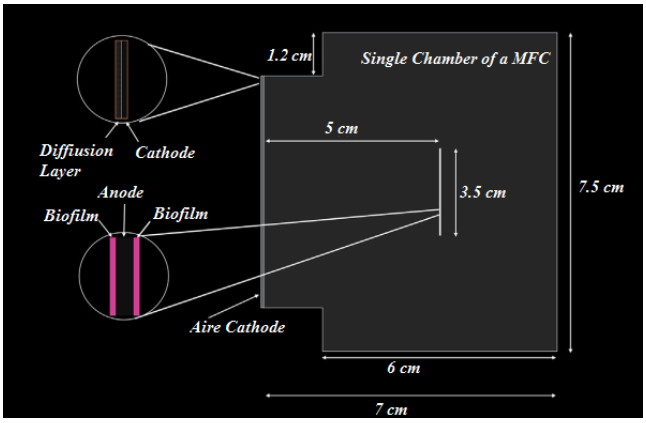

Figure 5. Schematic of the MFC including the air cathode.

Based on equations 1 and 2, the relationship between microbial growth and decay has been established by maintaining a steady-state biofilm of a given thickness. Acetate and CO_2 stay in the anodic electrode and cannot diffuse from the anode chamber to the cathode chamber. Meanwhile, the air phase could not diffuse into the anodic chamber; thus, acetate is the only electron donor substrate remaining in the analyte. A biofilm within a porous matrix can generate electrons by oxidizing substrates and delivering them to the anodic chamber. Since the biomass ingredients, including bacteria and extracellular polymeric substances (EPS), constitute the solid conducting phase, only the liquid analyte phase containing the substrate solution enters the porous biofilm matrix and is oxidized by the bacteria.

2.4. Numerical modeling.

Obviously, electrons transfer from the solid state, and the ions from the electrolyte phase, both obey Ohm's Law:

$$I = \sigma \nabla \varphi \; and \; i = \nabla I \quad (3)$$

Where "I" is the current density, σ is the conductivity, "φ" is the potential, and "I" is the current source.

The special current of electrons and ions in the case of porous chamber electrodes could be rearranged as:

$$i_s = \nabla I_s = \nabla(\sigma_{s,eff} \nabla \varphi_s \text{ and } i_l = \nabla I_l = \nabla(\sigma_{l,eff} \nabla \varphi_l \quad (4)$$

Where the subscripts "s" and "l" refer to the electrode phase and electrolyte phase, respectively. The effective amounts of conductivity (σ_{eff}) are calculated based on Bruggeman theory:

$$\sigma_{s,eff} = \in_s^{1.5} \sigma_s \text{ and } \sigma_{l,eff} = \in_l^{1.5} \sigma_l \quad (5)$$

Where $\in_s$ and $\in_l$ demonstrate the volume fraction of the electrode and electrolyte phase, respectively, current density in the porous biofilm is a function of biomass and substrate concentrations, as well as a function of overpotential. By assuming substrate consumption by bacteria obeying Monod kinetics, the charge-transfer kinetics at the anode can be rearranged as [54-57].

$$i_a = i_{0,a} \left(\frac{C_s}{C_s + K_{sa}}\right) C_x \exp\left(\frac{\alpha_a F \eta}{RT}\right) \quad (6)$$

Where, C_s is the substrate concentration, K_{sa} indicats the half-max rate of substrate and C_x is the anodic bacteria concentration. In addition, α_a is the anodic transfer coefficient and F is Faraday's constant. Meanwhile η is the overpotential and $i_{0,a}$ is the forward rate constant of the anode reaction. Since the air-cathode used in the microbial fuel cell is a gas diffusion electrode (GDE) that is inert to charge transfer, the current density at the cathode can be described using a concentration-dependent Butler-Volmer function as follows:

$$i_c = i_{0,c}\left(\exp\left[\frac{\alpha_c F \eta}{RT}\right] - \frac{C_{O_2}}{C_{O_2(ref)}} \exp\left[\frac{-(1-\alpha_c)F\eta}{RT}\right]\right) \quad (7)$$

Where, $i_{0,c}$ is the cathode reference, C_{O2} is the concentration of O_2, re, C_{O2}(ref) is the reference concentration of O_2, α_c cathodic transfer coefficient. Since the overpotential (η) is a function of electrode potential, it could be rearranged as:

$$\eta = \varphi_s - \varphi_l - E_{eq} \quad (8)$$

The gradient of substrate in the biofilm can be formulated by:

$$\nabla D_{eff,a} \nabla C_s = \frac{a_a i_a}{nF} \quad (9)$$

where, $D_{eff,a}$ is the effective diffusion coefficient, a_a is the active specific surface area of the anode, and is the number of electrons. Based on equation 10, since substrate cannot diffuse to the solid anodic chamber, a no-flux boundary condition is applied at the interface of the biofilm with the anodic electrode:

$$0 = D_{eff,a} \nabla C_s \quad (10)$$

The flux continuity condition (Eq. 11) is used at the interface of the outer surfaces of the biofilm with the analyte, assuming a concentration boundary layer of thickness 'L ' at the interface:

$$\frac{D_a}{L}\left(C_{s,bulk} - C_s\right) = D_{eff,a}\nabla C_s \quad (11)$$

Where, $C_{s,bulk}$ is the concentration and *Da* is the diffusion coefficient of the substrate.

3. Results and Discussion

3.1. Electricity production versus temperature and sample size.

Escherichia coli is a Gram-negative bacterium, generally used in both research laboratories and teaching centers. For this work, we grow it at 37°C under aerobic conditions. Since *E. coli* can grow over a wide pH range, we have grown it in Luria-Bertani broth, a rich liquid medium.

Besides the experiment, we also supposed that the natural temperature and the largest sample size, with a larger percentage of organic matter, would generate the most electricity. We use thermal limits between 0°C and 40°C; therefore, Experiments were accomplished for MFCs operating temperatures, 18°C, 23°C, 29°C, 37°C, and 40 °C. Related parameters were estimated through experimental results at 23°C, 29°C, and 37°C. The accuracy of the model parameters was later confirmed by comparing the experimental data of two other MFCs, operating at 20°C and 40°C. In the first series of experiments, the independent variable being studied was the type of those four bacteria present, *E. coli*, *Shewanella putrefaciens*, *Geobacter sulfurreducens*, and *Lactobacillus* (Figure 4) in related samples of the waste materials. We also fabricated our MFCs of these bacteria at room temperature (23°C) by measuring 3.0 cm × 3.0 cm × 4.0 cm dimensions for each type of sample. Therefore, 36 cm^3 volume of sample was used in each experiment for those four bacteria. For each sample, we measured electricity production using a digital multimeter within 5 minutes of MFC fabrication. Electricity production from several waste samples of various bacteria at 23°C is listed in Table 1. The measured amounts indicated that the MFC powered by the Lactobacillus waste sample produced the least electricity, and the MFC powered by the E. coli sample produced the most. *Lactobacillus* is a genus of Gram-positive facultative anaerobic or microaerophilic bacteria. The genus *Lactobacillus* is one of the major subgroups of the lactic acid bacteria, which convert lactose and other sugars into lactic acid. They are widely distributed and generally benign.

Table 3. Electricity production from several Waste samples of various bacteria at 23°C.

Waste sample	First trial (mV)	Second trial (mV)	Third trial (mV)	Percentage of each trial, respectively	Medium
E. coli	150	155	160	20%, 25%, 30%	155
Shewanella putrefaciens	146	144	147	15%, 16%, 17%	145.7
Geobacter sulfurreducens	140	145	142	18%, 19%, 20%	142.4
Lactobacillus	130	125	123	10%, 9%, 8%	126

Moreover, we completed several experiments through various percentages of organic matter in each of the waste samples. In the second test category, we selected two temperatures (0°C and 40°C) as the independent variable, while the dependent variable was electricity production in each MFC. In addition, for a better comparison among the results, we also used the room temperature (23°C). We created MFCs using topsoil and measuring 3.0 cm × 3.0 cm × 4.0 cm for each temperature. Table 4 presents the results of the experiments and indicates that electricity production was greatest at 0°C and lowest at 40°C. In addition, we tested

temperatures slightly above and below 0°C and 40°C. By this testing, we confirm that an MFC cannot function at temperatures at or below −8°C or temperatures at or above 46°C. On the low temperature end, electricity production increases from −4°C to −1°C and to 0°C, and then decreases from 0°C to 4°C and then to 5°C. Interestingly, 0°C is a peak for all samples.

Table 4. Electricity production according to various temperature ranges for 4 samples.

Temperature (°C)	*E. coli* (mV)	*Shewanella putrefaciens* (mV)	*Geobacter sulfurreducens* (mV)	*Lactobacillus* (mV)
-8	None	None	None	None
-4	45	38	32	30
-1	98	76	65	59
0	165	148	145	130
4	89	73	64	56
5	81	70	60	55
18	90	82	75	63
23	155	145.7	142.4	126
29	71	66	64	60
37	65	59	56	50
40	49	39	36	33
43	19	12	9	8
46	None	None	None	None

According to the data in Table 4, the electricity production uniformly decreases from 29°C to 37°C, 40°C, and finally 43°C. Because we were unable to control the temperature in the enclosed environment, we were also unable to test performance at temperatures very close to −8°C or 46°C. Thus, for the purpose of this study, we considered −8°C and 46°C the thermal limits for MFC designing.

In the third range of experiments, we tested the independent amounts of the anode chamber size as well as the type of sample that fills the chamber, 10.0 cm × 10.0 cm × 13.0 cm versus 2.0 cm × 2.0 cm × 4.0 cm. Consequently, the MFC of medium size measuring 3.0 cm × 3.0 cm × 4.0 cm was selected and fabricated for comparison with other sizes. Table 5 presents the measured data for each category of our tests, and we found that electricity production increases with sample size, whereas, in contrast to our expectations, the efficiency of electricity production decreases with sample size. The volume of the largest MFC is 36.11 times the volume of the medium MFC. Still, the electricity production of the largest MFC for E. coli is approximately 1.13 times that of the medium MFC. Similarly, the volume of the medium MFC is 2.25 times the volume of the smallest MFC. Still, the electricity production of the medium MFC is only 1.24 times the electricity production of the smallest MFC. Therefore, we found that the amount of electricity production does not depend on the sample size and power in the various MFCs, directly. Although electricity production increased with larger sample sizes, efficiency gradually decreased; therefore, an important conclusion was that simply increasing the MFC size may not be very effective due to diminishing returns.

Table 5. Electricity production versus sample size.

Anode chamber size	*E. coli* (mV)	*Shewanella putrefaciens* (mV)	*Geobacter sulfurreducens* (mV)	*Lactobacillus* (mV)
2.0 × 2.0 × 4.0	125	120	114	99
3.0 × 3.0 × 4.0	155	145 .7	142.4	126
10.0 × 10.0 × 13.0	175	159	152	131

3.2. Parameter estimation and model validation.

In this work, the COMSOL software, which enables coupled-physics simulations, was used for numerical calculations [57]. Parameter fitting regression analysis based on the Nelder-

Mead simplex optimization method was applied to estimate the model [11,12]. The target function was established based on theoretical and experimental data for power density as a function of current density. Figure 6 shows the experimental and fitted polarization at 23°C, 29°C, and 40°C, as reported in Table 4.

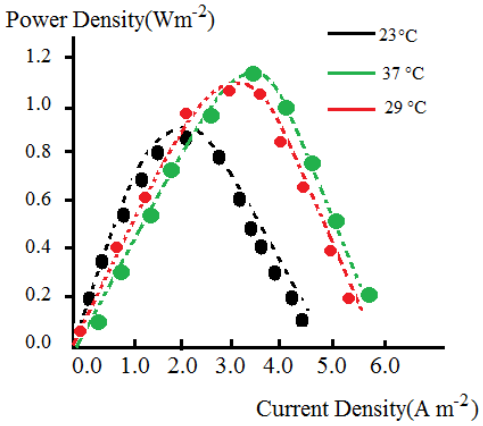

Figure 6. Power density vs current density for MFCs fabricated by E.coli at 23°C, 29°C, and 37°C; Experimental data are shown by solid color circles and numerical fitting is shown by dotted color line.

As shown, the numerical technique can be predicted by an accurate fitting to experimental data. The parameters obtained from fitting with the parameters that were obtained from experiments are also confirmed by other works. To prove our model's applicability in a wide range of temperatures, we used related parameter estimation compared with literature data. We found that this model can be applied to predict the power density of MFCs operating at temperatures above and below, using numerical fitting. Consequently, there is good agreement between the numerically calculated and experimental data, so the model's efficiency can be confirmed over a wide range of temperatures. It is notable that the model has a strong potential to predict the nonlinear trend in power density as a function of various temperatures. From the experimental data, we found that the power density of MFCs at various temperatures increases linearly between 23°C and 37°C; however, as the operating temperature increases, the power density begins to decrease. Both the experimental data and the numerical analysis have shown approximately 6% decrease in power density for an operating at 40°C compared to 37°C. These results were related to the deviation amounts of the power increase yielded during the enhancement temperature from 23°C to 37°C. Recent researchers have developed the influence of temperature on MFC performance [58-63]. Liu *et al*. [58], Feng *et al*. [59], and Min *et al*. [49, 61] all confirmed a linear relationship in power output vs temperature in 20°C to 32°C, 20°C to 30°C, and 22°C to 30°C. Larrosa-Guerrero *et al*. [63] also found a similar increase in power density vs temperatures from 4°C to 35°C. It is notable that in all previous studies, the maximum operating temperature is up to 35°C. We also studied the electrode spacing, Ionic strength, bacterial culture in biofilm, substrate composition, and its concentration. Obviously, an optimal correlation between power density and temperature cannot be achieved unless all other factors are accounted for simultaneously. This fact necessitates the use of numerical simulation to increase the efficiency of the electrical power in advanced MFCs. In addition, the current steady-state investigation, which couples the energy balance with the effect of temperature, can also be suitable for considering the influence of other physical parameters. The scope and capability of the numerical calculations could be investigated by power density changing as a function of ionic strength of the substrate and electrode distance. In addition, several recent studies on the performance of MFCs using

different sources of microorganisms have investigated waste materials, including Dairy Industry Waste Water (DIWW), Dyeing Waste Water (DWW-2), and Cow Dung, which were used as sources of microorganisms [64-77].

3.3. Ionic strength effects.

We studied electrolyte conductivity (σ_I) and the effect of ionic strength for the substrate solution on the MFC efficiency (equations 3-5). As can be seen in Figure 7, the highest power density initially increases linearly versus electrolyte conductivity between 0.12 W m^{-2} at σ_I = $1e^{-4}$ Sm^{-1} to 1.1 W m^{-2} for $\sigma_I = 1e^{-2}$ Sm^{-1}. Then, by enhancing conductivity, the power density gradually decreases towards $\sigma_I = 2e^{-1}$ Sm^{-1}. These results confirm our experimental data on the power density of the ionic strength from several bacterial substrates, where an increase in conductivity does not result in any further improvement in power density.

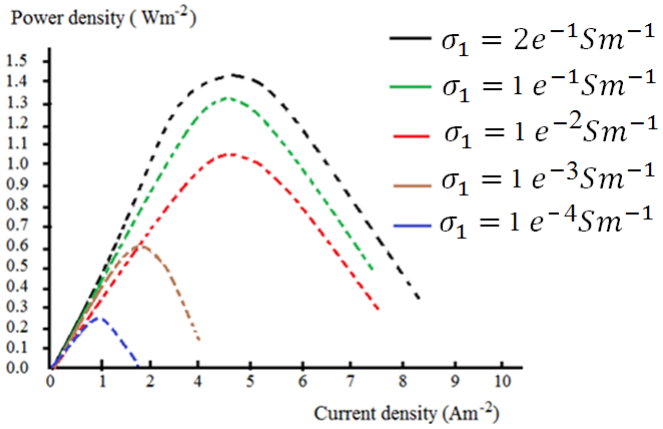

Figure 7. Power density of the *E.coli* system in various conductivities vs current density.

In Table 6, the ionic strength effects for *E. coli*, *Shewanella putrefaciens*, *Lactobacillus*, and *Geobacter* sulfurreducens are listed, both experimentally and numerically.

Table 6. Electricity production from several waste samples of various bacteria at 23°C.

Waste sample/distance		Electrolyte conductivity (σ_I) with Power density = 1.1 Wm^{-2}				
		$2e^{-1}$ Sm^{-1}	$1e^{-1}$ Sm^{-1}	$1e^{-2}$ Sm^{-1}	$1e^{-3}$ Sm^{-1}	$1e^{-4}Sm^{-1}$
E. coli	experimental	1.4	1.3	1.0	0.6	0.2
	numerical	1.35	1.33	0.95	0.65	0.25
Shewanella putrefaciens	experimental	1.35	1.15	0.90	0.6	0.18
	numerical	1.25	1.05	0.85	0.55	0.2
Geobacter sulfurreducens	experimental	1.2	1.0	0.85	0.58	0.15
	numerical	1.25	0.95	0.88	0.55	0.15
Lactobacillus	experimental	1.15	0.9	0.8	0.55	0.12
	numerical	1.1	0.9	0.8	0.58	0.1

3.4. Electrode chambers structural size effect.

Since conductivity reflects the rate of ion transfer, higher conductivity promotes ionic conduction, thereby reducing Ohmic losses and power output in MFCs. The effects of electrode chamber structural size and the inter-electrode distance between the anode and cathode have been investigated for *E. coli*, *Shewanella putrefaciens*, *Lactobacillus*, and *Geobacter sulfurreducens*. Inter-electrode distances were varied from 1 cm to 5cm. In all items, maximum power density increases as the distance between the two electrodes is decreased. Based on our experimental results and numerical studies, in general, as the inter-electrode distance decreased, the internal resistance also decreased. The effect of electrode distance also depends

on the ionic strength change of the solution. It was observed that when electrolytes with conductivities more than 0.02 S m^{-1} were used, decreasing the electrode spacing does not result in any significant gain in power output, but power output changes with electrolyte conductivity smaller than 0.02 S m^{-1}. With electrolyte conductivity equal to 0.01 S m^{-1}, we calculated approximately a 10% increase in power output by reducing the distance from 5 cm to 1 cm. Moreover, using an electrolyte with a weak ionic strength equal to $\sigma_I = 1e^{-4}$ S m^{-1}, maximum power density changes from 0.7 Wm^{-2} towards 1.3 Wm^{-2} during reducing distance from 5 cm to 1 cm (Figure 8).

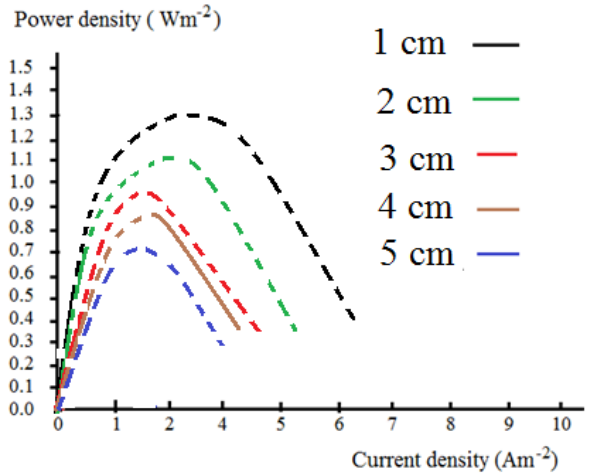

Figure 8. Power density of *E.coli* system in various distances vs current density with electrolyte conductivity = 0.01 S m^{-1}.

In Table 7, the distance effect for *E. coli*, *Shewanella putrefaciens*, *Lactobacillus*, and *Geobacter sulfurreducens* has been listed both in experimental and numerical calculations.

Table 7. Electricity production from several waste samples of various bacteria at 23°C.

Waste sample/distance		Power density (Wm^{-2}) with conductivity = 0.01 S m^{-1} and $\sigma_I = 1e^{-4}$ S m^{-1}				
		1 cm	2 cm	3 cm	4 cm	5 cm
E. coli	experimental	1.3	1.1	0.95	0.85	0.7
	numerical	1.35	0.9	0.9	0.80	0.75
Shewanella putrefaciens	experimental	1.25	1.05	0.90	0.8	0.65
	numerical	1.2	1.0	0.85	0.75	0.7
Geobacter sulfurreducens	experimental	1.2	1.0	0.85	0.75	0.6
	numerical	1.25	1.1	0.9	0.80	0.65
Lactobacillus	experimental	1.2	0.9	0.8	0.7	0.55
	numerical	1.1	0.95	0.8	0.75	0.6

4. Conclusions

This work clearly shows the effects of temperature and cell dimensions on MFC efficiency, in agreement with the experimental data. The two-dimensional analysis enables us to examine ionic changes, including electronic current densities, as well as local reaction rates in the two cathodic and anodic chambers. According to this work, a method has been defined for numerical calculations that allows us to explain the non-linear trend in efficiency with temperature. It is also discussed that all parameters are interlinked and are essential for obtaining a realistic definition of MFC efficiency. This mathematical simulation is a general model that can be applied to various MFC configurations due to its fast convergence and quick optimization. Our mathematical approach is related to the following hypothesis: 1- The biofilm was constructed on a solid, porous, conductive matrix and was controlled with a fixed conductivity and pH. 2- Addition of substrate was supposed to be identical, mixed in the

analyte, and the substrate gradient only occurs in the biofilm. 3- A concentration boundary layer exists between the biofilm matrix and the analyte. In addition, for future work, they can be properly applied to study dynamic efficiency over time. In addition, the scope of this model extends beyond temperature studies in various MFCs and can also be used for other parametric studies, such as ionic strength, dimensions, ionic conductivities, and electronic currents.

Author Contributions

Conceptualization, M.M. and E.F.; methodology, M.M.; software, F.M.and M.R.; validation, E.F. and M.M., M.R.; formal analysis, M.M.; investigation, M.M.; resources, E.F.and M.R.; data curation, E.F.; writing—original draft preparation, F.M.; writing—review and editing, M.M.and E.F.; visualization, E.F.and M.R.; supervision, M.M.; project administration, M.M.; funding acquisition, M.M. All authors have read and agreed to the published version of the manuscript."

Institutional Review Board Statement

Not applicable.

Informed Consent Statement

Not applicable.

Data Availability Statement

Data supporting the findings of this study are available upon reasonable request from the corresponding author.

Funding

This research received no external funding.

Acknowledgments

The authors thank Kastamonu University in Turkey and I.A.U. University of Iran for their support.

Conflicts of Interest

The authors declare no conflict of interest.

Abbreviations

The following abbreviations are used in this manuscript:

Abbreviation	Definition
MFCs	microbial fuel cells
PEM	proton exchange membranes
EAB	electrochemically active bacteria
AEM	anion exchange membrane
CEM	cation exchange membrane
DIWW	Dairy Industry Waste Water
DWW	Dyeing Waste Water

References

1. Al-Asheh, S.; Al-Assaf, Y.; Aidan, A. Single-chamber microbial fuel cells' behavior at different operational scenarios. *Energies* **2020**, *13*, 5458, https://doi.org/10.3390/en13205458.
2. Kiaeenajad, A.; Moqtaderi, H.; Mahmoodi, N.; Maerufi, S. Design and Construction of a Microbial Fuel Cell for Electricity Generation from Municipal Wastewater Using Industrial Vinasse as Substrate. *Mod. Mech. Eng.* **2020**, *20*, 2403-2412.
3. Ni, H.; Wang, K.; Lv, S.; Wang, X.; Zhuo, L.; Zhang, J. Effects of concentration variations on the performance and microbial community in microbial fuel cell using swine wastewater. *Energies* **2020**, *13*, 2231, https://doi.org/10.3390/en13092231.
4. Tan, S.M.; Ong, S.A.; Ho, L.N.; Wong, Y.S.; Thung, W.H.; Teoh, T.P. The reaction of wastewater treatment and power generation of single chamber microbial fuel cell against substrate concentration and anode distributions. *J. Environ. Health Sci. Eng.* **2020**, *18*, 793-807, https://doi.org/10.1007/s40201-020-00504-w.
5. Saravanan, P. Microbial fuel cell: a prospective sustainable solution for energy and environmental crisis. *Int. J. Biosens. Bioelectron.* **2018**, *4*, 191–193.
6. Yuan, H.; Hou, Y.; Abu-Reesh, I.M.; Chen, J.; He, Z. Oxygen reduction reaction catalysts used in microbial fuel cells for energy-efficient wastewater treatment: a review. *Mater. Horiz.* **2016**, *3*, 382–401, https://doi.org/10.1039/c6mh00093b.
7. Kalathil, S.; Nguyen, V.H.; Shim, J.J.; Khan, M.M.; Lee, J.; Cho, M.H. Enhanced performance of a microbial fuel cell using CNT/MnO_2 nanocomposite as a bio anode material. *J. Nanosci. Nanotechnol*. **2013**, *13*, 7712–7716, https://doi.org/10.1166/jnn.2013.7832.
8. Gabisa, E.W.; Gheewala, S.H. Potential of bio-energy production in Ethiopia based on available biomass residues. *Biomass Bioenergy* **2018**, *111*, 77–87, https://doi.org/10.1016/j.biombioe.2018.02.009.
9. Monajjemi, M., Naderi, F., Mollaamin, F., Khaleghian, M, Drug design outlook by calculation of second virial coefficient as a nano study. j*ournal of the Mexican Chemical Society*, **2012**, *56(2)*, 207–211, https://doi.org/10.29356/jmcs.v56i2.323
10. Monajjemi, M.; Mollaamin, F.; Shahriari, S.; Khalaj, Z.; Sakhaeinia, H.; Alihosseini, A. Interaction of Nano-Boron Nitride Sheets with Electrodes in Lithium Ion Battery for Increasing Voltage and Amperage. *Russ. J. Phys. Chem. B.* **2024**, *18*, 1090–1112, https://doi.org/10.1134/S1990793124700465.
11. Monajjemi, M.; Mohammadi, S.; Shahriari, S.; Mollaamin, F. Experimental and Theoretical Studies of ZnO Nanotubes: an Approach to Chemical Physics Characterization of ZnONTs, Including Morphology, Piezoelectric, and Density of States. *Russ. J. Phys. Chem. B.* **2024**, *18*, 308–324, https://doi.org/10.1134/S1990793124010342.
12. Gadkari, S.; Gu, S.; Sadhukhan, J. Two-dimensional mathematical model of an air-cathode microbial fuel cell with graphite fiber brush anode. *J. Power Sources* **2019**, *441*, 227145, https://doi.org/10.1016/j.jpowsour.2019.227145.
13. Shahriari, S.; Soofi, N.S.; Farzi, F.; Attarikhasraghi, N.; Khosravi, S.; Babaei Tuskiee, B.B.; Esmkhani, R.; Monajjemi, M. Interaction of nano-boron nitride/graphene sheets with anode lithium ion battery. J. Comput. Theor. Nanosci. **2016**, *13*, 3070-3082, https://doi.org/10.1166/jctn.2016.4959.
14. Evelyn; Saputra, E.; Amri, A.; Marshall, A.; Gostomski, P. Reaction kinetics for microbial-reduced mediator in an ethanol-fed microbial fuel cell. *MATEC Web Conf.* **2019**, *276*, 06010, https://doi.org/10.1051/matecconf/201927606010.
15. Worku, A.; Tefera, N.; Kloos, H.; Benor, S. Bioremediation of brewery wastewater using hydroponics planted with vetiver grass in Addis Ababa, Ethiopia. *Bioresour. Bioprocess* **2018**, *5*, 39, https://doi.org/10.1186/s40643-018-0225-5.
16. Chen, J.; Wang, Y.; He, X.; Xu, S.; Fang, M.; Zhao, X.; Shang, Y. Electrochemical properties of MnO_2 nanorods as anode materials for lithium ion batteries. *Electrochim. Acta* **2014**, *142*, 152–156, https://doi.org/10.1016/j.electacta.2014.07.089.
17. Jia, M.; Zhang, Z.; Li, J.; Ma, X.; Chen, L.; Yang, X. Molecular imprinting technology for microorganism analysis. *TrAC – Trends Anal. Chem.* **2018**, *106*, 190–201, https://doi.org/10.1016/j.trac.2018.07.011.
18. Aryal, N.; Ammam, F.; Patil, S.A.; Pant, D. An overview of cathode materials for microbial electrosynthesis of chemicals from carbon dioxide. *Green Chem.* **2017**, *19*, 5748–5760, https://doi.org/10.1039/c7gc01801k.
19. Vidali, M.; Bioremediation. An overview. *Pure Appl. Chem*. **2001**, *73*, 1163–1172, https://doi.org/10.1351/pac200173071163.

20. Santoro, C.; Arbizzani, C.; Erable, B.; Ieropoulos, I.; Microbial fuel cells: From fundamentals to applications. A review. *J. Power Sources* **2017**, *356*, 225–244, https://doi.org/10.1016/j.jpowsour.2017.03.109.
21. Tartakovsky, B.; Guiot, S.R. A comparison of air and hydrogen peroxide oxygenated microbial fuel cell reactors. *Biotechnol. Prog.* **2006**, *22*, 241-246, https://doi.org/10.1021/bp050225j.
22. Cao, C.; Wang, H.; Liu, W.; Liao, X.; Li, L. Nafion membranes as electrolyte and separator for sodium-ion battery. *Int. J. Hydrogen Energy* **2014**, *39*, 16110-16115, https://doi.org/10.1016/j.ijhydene.2013.12.119.
23. Koók, L.; Nemestóthy, N.; Bélafi-Bakó, K.; Bakonyi, P.Treatment of dark fermentative H2 production effluents by microbial fuel cells: A tutorial review on promising operational strategies and practices. *Int. J. Hydrogen Energy* **2021**, *46*, 5556–5569, https://doi.org/10.1016/j.ijhydene.2020.11.084.
24. Zuo, Y.; Cheng, S.; Logan, B.E. Ion exchange membrane cathodes for scalable microbial fuel cells. *Environ. Sci. Technol*. **2008**, *4218*, 6967–6972, https://doi.org/10.1021/es801055r.
25. Thomas, O.D.; Soo, K.J.W.Y.; Peckham, T.J.; Kulkarni, M.P.; Holdcroft, S. A Stable Hydroxide-Conducting Polymer. *J. Am. Chem. Soc.* **2012**, *134*, 10753–10756, https://doi.org/10.1021/ja303067t.
26. Hassan, N.U.; Motyka, E.; Kweder, J.; Ganesan, P.; Brechin, B.; Zulevi, B.; Col ón-Mercado, H.R.; Kohl, P.A.; Mustain, W.E. Effect of porous transport layer properties on the anode electrode in anion exchange membrane electrolyzers. *J. Power Sources* **2023**, *555*, 232371, http://dx.doi.org/10.2139/ssrn.4219578.
27. Wang, J.; Zhao, Y.; Setzler, B.P.; Rojas-Carbonell, S.; Ben Yehuda, C.; Amel, A.; Page, M.; Wang, L.; Hu, K.; Shi, L.; Gottesfeld, S.; Xu, B.; Yan, Y. Poly(aryl piperidinium) membranes and ionomers for hydroxide exchange membrane fuel cells. *Nat. Energy* **2019**, *4*, 392–398, https://doi.org/10.1038/s41560-019-0372-8.
28. Truong, V.M.; Yang, M.-K.; Yang, H. Functionalized Carbon Black Supported Silver (Ag/C) Catalysts in Cathode Electrode for Alkaline Anion Exchange Membrane Fuel Cells. *Int. J. Precis. Eng. Manuf.-Green Technol.* **2019**, *6*, 711–721, https://doi.org/10.1007/s40684-019-00123-3.
29. Lee, W.-H.; Park, E.J.; Han, J.; Shin, D.W.; Kim, Y.S.; Bae, C. Poly(terphenylene) Anion Exchange Membranes: The Effect of Backbone Structure on Morphology and Membrane Property. *ACS Macro Lett.* **2017**, *6*, 566–570, https://doi.org/10.1021/acsmacrolett.7b00148.
30. Marinkas, A.; Struźyńska-Piron, I.; Lee, Y.; Lim, A.; Park, H.S.; Jang, J.H.; Kim, H.-J.; Kim, J.; Maljusch, A.; Conradi, O. Anion-conductive membranes based on 2-mesityl-benzimidazolium functionalised poly (2, 6-dimethyl-1, 4-phenylene oxide) and their use in alkaline water electrolysis. *Polymer* **2018**, *145*, 242-251, https://doi.org/10.1016/j.polymer.2018.05.008.
31. Mollaamin, F.; Monajjemi, M. Nanomaterials for Sustainable Energy in Hydrogen-Fuel Cell: Functionalization and Characterization of Carbon Nano-Semiconductors with Silicon, Germanium, Tin or Lead through Density Functional Theory Study. *Russ. J. Phys. Chem. B* **2024**, *18*, 607–623, https://doi.org/10.1134/S1990793124020271.
32. Mollaamin, F.; Shahriari, S.; Monajjemi, M. Influence of Transition Metals for Emergence of Energy Storage in Fuel Cells through Hydrogen Adsorption on the MgAl Surface. *Russ. J. Phys. Chem. B* **2024**, *18*, 398–418, https://doi.org/10.1134/S199079312402026X.
33. Mollaamin, F.; Monajjemi, M. Electric and Magnetic Evaluation of Aluminum–Magnesium Nanoalloy Decorated with Germanium Through Heterocyclic Carbenes Adsorption: A Density Functional Theory Study. *Russ. J. Phys. Chem. B.* **2023**, *17*, 658–672, https://doi.org/10.1134/S1990793123030223.
34. Baudler, A.; Schmidt, I.; Langner, M.; Greiner,A.; Schröder, U. Does it has to be carbon? Metal anodes in microbial fuel cells and related bioelectrochemical systems. *Energy Environ. Sci.* **2015**, *8*, 2048–2055, https://doi.org/10.1039/C5EE00866B.
35. Qiao, Y.; Li, C.M.; Bao, S.J.; Bao, Q.L. Carbon nanotube/polyaniline composite as anode material for microbial fuel cells. *J. Power Sources* **2007**, *170*, 79–84, https://doi.org/10.1016/j.jpowsour.2007.03.048.
36. Marshall, C.W.; Ross, D.E.; Fichot, E.B.; Norman, R.S.; May, H.D. Long-term operation of microbial electrosynthesis systems improves acetate production by autotrophic microbiomes. *Environ. Sci. Technol.* **2013**, *47*, 6023–6029, https://doi.org/10.1021/es400341b.
37. Potter, M.C. Electrical effects accompanying the decomposition of organic compounds. *Proc. R. Soc. B Biol. Sci.* **1911**, *84*, 260–276, https://doi.org/10.1098/rspb.1911.0073.
38. Jung, S.; Regan, J.M. Comparison of anode bacterial communities and performance in microbial fuel cells with different electron donors. *Appl. Microbiol. Biotechnol.* **2007**, *77*, 393–402, https://doi.org/10.1007/s00253-007-1162-y.
39. Reguera, G.; Nevin, K.P.; Nicoll, J.S.; Covalla, S.F.; Woodard, T.L.; Lovley, D.R. Biofilm and nanowire production leads to increased current in Geobacter sulfurreducens fuel cells. *Appl. Environ. Microbiol.* **2006**, *72*, 7345–7348, https://doi.org/10.1128/AEM.01444-06.

40. Ringeisen, B.R.; Henderson, E.; Wu, P.K.; Pietron, J.; Ray, R.; Little, B.; Biffinger, J.C.; Jones-Meehan, J.M. High power density from a miniature microbial fuel cell using Shewanella oneidensis DSP10. *Environ. Sci. Technol.* **2006**, *40*, 2629-2634, https://doi.org/10.1021/es052254w.
41. Kim, H.J.; Moon, S.H.; Chang, I.S.; BYUNG, H.K. A microbial fuel cell type lactate biosensor using a metal-reducing bacterium, Shewanella putrefaciens. *J. Microbiol. Biotechnol.* **1999**, *9*, 365-367.
42. Grzebyk, M.; Poźniak, G. Microbial fuel cells (MFCs) with interpolymer cation exchange membranes. *Sep. Purif. Technol.* **2004**, *41*, 321-328, https://doi.org/10.1016/j.seppur.2004.04.009.
43. Park, H.S.; Kim, B.H.; Kim, H.S.; Kim, H.J.; Kim, G.T.; Kim, M.; Chang, I.S.; Park, Y.K.; Chang, H.I. A novel electrochemically active and Fe (III)-reducing bacterium phylogenetically related to Clostridium butyricum isolated from a microbial fuel cell. *Anaerobe* **2001**, *7*, 297-306, https://doi.org/10.1006/anae.2001.0399.
44. Rabaey, K.; Boon, N.; Höfte, M.; Verstraete,W. Microbial phenazine production enhances electron transfer in biofuel cells. *Environ. Sci. Technol*. **2005**, *39*, 3401–3408, https://doi.org/10.1021/es048563o.
45. Lee, S.A.; Choi, Y.; Jung, S.; Kim, S. Effect of initial carbon sources on the electrochemical detection of glucose by Gluconobacter oxydans. *Bioelectrochemistry* **2002**, *57*, 173–178, https://doi.org/10.1016/s1567-5394(02)00115-9.
46. Bond, D.R.; Lovley, D.R. Evidence for Involvement of an Electron Shuttle in Electricity Generation by Geothrix fermentans Evidence for Involvement of an Electron Shuttle in Electricity Generation by Geothrix fermentans. *Appl. Environ. Microbiol*. **2005**, *71*, 2186–2189, https://doi.org/10.1128/AEM.71.4.2186-2189.2005.
47. Zhang, Y.; Noori, J.S.; Angelidaki, I. Simultaneous organic carbon, nutrients removal and energy production in a photomicrobial fuel cell (PFC). *Energy Environ. Sci.* **2011**, *4*, 4340–4346, https://doi.org/10.1039/C1EE02089G.
48. Lakaniemi, A.-M.; Tuovinen, O.H.; Puhakka, J.A. Production of electricity and butanol from microalgal biomass in microbial fuel cells. *BioEnergy Res.* **2012**, *5*, 481-491, https://doi.org/10.1007/s12155-012-9186-2.
49. Kakarla, R.: Min, B.Evaluation of microbial fuel cell operation using algae as an oxygen supplier: carbon paper cathode vs. carbon brush cathode. *Bioprocess Biosyst. Eng*. **2014**, *37*, 2453–2461, https://doi.org/10.1007/s00449-014-1223-4.
50. Fan, Z.; Li, J.; Zhou, Y.; Fu, Q.; Yang, W.; Zhu, X.; Liao, Q. A green, cheap, high-performance carbonaceous catalyst derived from Chlorella pyrenoidosa for oxygen reduction reaction in microbial fuel cells. *Int. J. Hydrogen Energy* **2017**, *42*, 27657-27665, https://doi.org/10.1016/j.ijhydene.2017.07.177.
51. Wu, C.; Liu, X.-W.; Li, W.-W.; Sheng, G.-P.; Zang, G.-L.; Cheng, Y.-Y.; Shen, N.; Yang, Y.-P.; Yu, H.-Q. A white-rot fungus is used as a biocathode to improve electricity production of a microbial fuel cell. *Appl. Energy* **2012**, *98*, 594-596, https://doi.org/10.1016/j.apenergy.2012.02.058.
52. Gal, I.; Schlesinger, O.; Amir, L.; Alfonta, L. Yeast surface isplay of dehydrogenases in microbial fuelcells. *Bioelectrochemistry* **2016**, *112*, 53–60, https://doi.org/10.1016/j.bioelechem.2016.07.006.
53. Vega, C.L.C.; Fernandez, I. Mediating Effect of Ferric Chelate Compounds in Microbial Fuel-Cells With LLactobacillus Plantarum, Streptococcus-Lactis, and Erwinia Dissolvens. *Bioelectrochem. Bioenerg*. **1987**, *17*, 217–222, https://doi.org/10.1016/0302-4598(87)80026-0.
54. Rabaey, K.; Van de Sompel, K.; Maignien, L.; Boon, N.; Aelterman, P.; Clauwaert, P.; De Schamphelaire, L.; Pham, H.T.; Vermeulen, J.; Verhaege, M. Microbial fuel cells for sulfide removal. *Environ. Sci. Technol.* **2006**, *40*, 5218-5224, https://doi.org/10.1021/es060382u.
55. Mollaamin, F.; Monajjemi, M. Graphene-based resistant sensor decorated with Mn, Co, Cu for nitric oxide detection: Langmuir adsorption & DFT method. *Sensor Review* **2023**, *43*, 266–279, https://doi.org/10.1108/SR-03-2023-0040.
56. Mollaamin, F.; Monajjemi, M. Doping of Graphene Nanostructure with Iron, Nickel and Zinc as Selective Detector for the Toxic Gas Removal: A Density Functional Theory Study. *C* **2023**, *9*, 20, https://doi.org/10.3390/c9010020.
57. Gadkari, S.; Fidalgo, B.; Gu, S. Numerical investigation of microwave-assisted pyrolysis of lignin. *Fuel Process. Technol.* **2017**, *156*, 473-484, https://doi.org/10.1016/j.fuproc.2016.10.012.
58. Liu, H.; Cheng, S.; Logan, B.E. Power generation in fed-batch microbial fuel cells as a function of ionic strength, temperature, and reactor configuration. *Environ. Sci. Technol*. **2005**, *39*, 5488–5493, https://doi.org/10.1021/es050316c.
59. Feng, Y.; Wang, X.; Logan, B.E.; Lee, H. Brewery wastewater treatment using air cathode microbial fuel cells. *Appl. Microbiol. Biotechnol*. **2008**, *78*, 873–880, https://doi.org/10.1007/s00253-008-1360-2.
60. Patil, S.A.; Harnisch, F.; Kapadnis, B.; Schröder, U. Electroactive mixed culture biofilms in microbial bioelectrochemical systems: the role of temperature for biofilm formation and performance. *Biosens. Bioelectron.* **2010**, *26*, 803-808, https://doi.org/10.1016/j.bios.2010.06.019.

61. Min, B.; Román, O.B.; Angelidaki, I. Importance of temperature and anodic medium composition on microbial fuel cell (mfc) performance. *Biotechnol. Lett.* **2008**, *30*, 1213–1218, https://doi.org/10.1007/s10529-008-9687-4.
62. Mollaamin, F.; Monajjemi, M. Adsorption ability of Ga_5N10 nanomaterial for removing metal ions contamination from drinking water by DFT. *Int. J. Quantum Chem.* **2024**, *124*, e27348, https://doi.org/10.1002/qua.27348.
63. Larrosa-Guerrero, K.; Scott, I.M.; Head, F.; Mateo, A.; Ginesta, C.; Godinez, S.C. Effect of temperature on the performance of microbial fuel cells. *Fuel* **2010**, *89*, 3985–3994, https://doi.org/10.3303/CET1021078.
64. Rial, R.C. Biofuels versus Climate Change: Exploring Potentials and Challenges in the Energy Transition. *Renew. Sustain. Energy Rev.* **2024**, *196*, 114369, https://doi.org/10.1016/j.rser.2024.114369.
65. Irham, A.; Roslan, M.F.; Jern, K.P.; Hannan, M.A.; Mahlia, T.M.I. Hydrogen Energy Storage Integrated Grid: A Bibliometric Analysis for Sustainable Energy Production. *Int. J. Hydrogen Energy* **2024**, *63*, 1044–1087, https://doi.org/10.1016/j.ijhydene.2024.03.235.
66. Goren, A.Y.; Dincer, I.; Gogoi, S.B.; Boral, P.; Patel, D. Recent Developments on Carbon Neutrality through Carbon Dioxide Capture and Utilization with Clean Hydrogen for Production of Alternative Fuels for Smart Cities. *Int. J. Hydrogen Energy* **2024**, *79*, 551–578, https://doi.org/10.1016/j.ijhydene.2024.06.421.
67. Gupta, S.; Patro, A.; Mittal, Y.; Dwivedi, S.; Saket, P.; Panja, R.; Saeed, T.; Martínez, F.; Yadav, A.K. The Race between Classical Microbial Fuel Cells, Sediment-Microbial Fuel Cells, Plant-Microbial Fuel Cells, and Constructed Wetlands-Microbial Fuel Cells: Applications and Technology Readiness Level. *Sci. Total Environ.* **2023**, *879*, 162757, https://doi.org/10.1016/j.scitotenv.2023.162757.
68. Kwofie, M.; Amanful, B.; Gamor, S.; Kaku, F. Comprehensive Analysis of Clean Energy Generation Mechanisms in Microbial Fuel Cells. *Int. J. Energy Res.* **2024**, *2024*, 5866657, https://doi.org/10.1155/2024/5866657.
69. Arun, J.; SundarRajan, P.; Pavithra, K.G.; Priyadharsini, P.; Shyam, S.; Goutham, R.; Le, Q.H.; Pugazhendhi, A. New Insights into Microbial Electrolysis Cells (MEC) and Microbial Fuel Cells (MFC) for Simultaneous Wastewater Treatment and Green Fuel (Hydrogen) Generation. *Fuel* **2024**, *355*, 129530, https://doi.org/10.1016/j.fuel.2023.129530.
70. Parwate, S.A.; Xue, W.; Koottatep, T.; Salam, A. Organic Waste for Bioelectricity Generation in Microbial Fuel Cells: Effects of Feed Physicochemical Characteristics. *Processes* **2024**, *12*, 1110, https://doi.org/10.3390/pr12061110.
71. Zapata-Martínez, O.; Villa-Gomez, D.; Tapia-Tussell, R.; Dominguez-Maldonado, J.; Hernández-Zárate, G.; España-Gamboa, E.; Valdez-Ojeda, R.; Alzate-Gaviria, L. Craft Brewery Wastewater Treatment in a Scalable Microbial Fuel Cell Stack. *Beverages* **2024**, *10*, 20, https://doi.org/10.3390/beverages10010020.
72. Fuku, X.; Modibedi, M. Performance of $BiCu_2O$ Modified Pd/C as an Anode Electrocatalyst for Direct Ethanol Fuel Cell System. *Catal. Today* **2024**, *425*, 114305, https://doi.org/10.1016/j.cattod.2023.114305.
73. Karuga, J.; Fuku, X.; Nkambule, T.; Mamba, B.; Kebede, M.A. Advances in Mitigating Oxygen Evolution, Phase Transformation, and Voltage Fading in Li/Mn-Rich Cathode Materials via Cationic Doping and Surface Modification. *J. Energy Storage* **2024**, *98*, 113144, https://doi.org/10.1016/j.est.2024.113144.
74. Adhikari, B.; Safaee Chalkasra, L.S. Mobilizing Private Sector Investment for Climate Action: Enhancing Ambition and Scaling up Implementation. *J. Sustain. Financ. Invest.* **2023**, *13*, 1110–1127, https://doi.org/10.1080/20430795.2021.1917929.
75. Niloofar, P.; Lazarova-Molnar, S.; Thumba, D.A.; Shahin, K.I. A Conceptual Framework for Holistic Assessment of Decision Support Systems for Sustainable Livestock Farming. *Ecol. Indic.* **2023**, *155*, 111029, https://doi.org/10.1016/j.ecolind.2023.111029.
76. Musarat, M.A.; Irfan, M.; Alaloul, W.S.; Maqsoom, A.; Ghufran, M. A Review on the Way Forward in Construction through Industrial Revolution 5.0. *Sustainability* **2023**, *15*, 13862, https://doi.org/10.3390/su151813862.
77. Kabir, M.M.; Akter, M.M.; Huang, Z.; Tijing, L.; Shon, H.K. Hydrogen Production from Water Industries for a Circular Economy. *Desalination* **2023**, *554*, 116448, https://doi.org/10.1016/j.desal.2023.116448.

Publisher's Note & Disclaimer